Spectroscopic Analyses and the Influence of Concentration on the Photoluminescence Characteristics of Sm^{+3}-Doped Silica Sol-Gel matrix

Amenah A. Salman*, Firas Jawad Kadhim
Department of Physics, College of Science, University of Baghdad, Baghdad, Iraq

Abstract:

The sol-gel route is used to prepare samarium (Sm^{+3}) ions doped in silica monoliths as a function of active ion concentrations up to 0.0178%. The spectroscopic activity of Sm^{+3} ions doped-silica matrices is investigated using UV-Visible spectroscopy and photoluminescence spectroscopy. $^{4}G_{5/2}$ emissions are observed from a minority of isolated Sm^{+3} ions within the pores structure of silica matrix, UV-Vis spectra reveals absorption peaks due to Sm^{+3} active centers. X-ray diffraction and FTIR results support the distribution of such ions in these porous. Analysis indicates that at high doping levels, most ions reside in clusters and $^{4}G_{5/2}$ emission, which is demonstrated by the quenching processes observed in the corresponding spectra. Some spectroscopic parameters such as emission cross-section and oscillator strength are determined and analyzed.

Keywords: Sol-gel; Lanthanide ions spectroscopy, photo luminesces Sm^{+3}

التحليل الطيفي وتاثير التركيز على الخصائص الانبعاثيه الضوئيه لمصفوفات السليكا المطعمه بايونات السماريوم

امنه علي سلمان*، فراس جواد كاظم

قسم الفيزياء،كليه العلوم،جامعه بغداد،بغداد،العراق

الخلاصه:

تم استخدام طريقة Sol–gel لتحضير أيونات السماريوم المطعمه في مصفوفات السيليكا كدالة لتراكيز مختلفه لغايه 0.0178٪ من ايونات السماريوم. تم التحقق من الفعاليه الطيفيه لمصفوفات السيليكا المطعمه بايونات السماريوم باستخدام التحليل الطيفي ضمن المدى الفوق بنفسجي /مرئي . لوحظت الانبعاثات الحاصلة من مستوي $^{4}G_{5/2}$ لمجاميع أيونات السماريوم داخل المسامات التركيبيه لمصفوفة السيليكا ، وتوضح اطياف الامتصاص ضمن المدى الفوق بنفسجي/مرئي قمم الامتصاص الناتجه عن ايونات السماريوم ،نتائج حيود الأشعة السينية ومطيافية الاشعة تحت الحمراء تدعم توزيع الأيونات داخل المسامات التركيبية. يشير التحليل إلى أنه عند مستويات التطعيم العاليه ، اغلب الأيونات توجد بمجاميع والانبعاثات الحاصله من مستوي $^{4}G_{5/2}$ ، ويظهرمن خلال عمليات الاخماد الواضحه في الأطياف. تم حساب وتحليل بعض المعلمات الطيفية مثل المقطع العرضي للانبعاث وشدة التذبذب لانتقالات ايونات السماريوم.

*Email: amina.ali1104a@sc.uobaghdad.edu.iq

Introduction:

The interest in luminescent materials containing samarium ions (Sm^{+3}) is relatively recent and rapidly growing due to the properties that make it peculiar in the panorama of the lanthanide series and its attractive applications, such as temperature sensing optical fiber, optical data storage, optical fiber communication, solid-state materials emitting visible light (near white light emitting diode LEDs) due to 4f–4f and 4f– 5d electronic transitions [1−3]. In the visible and ultraviolet spectral regions, white light-emitting diodes (W-LEDs) produce white light by employing phosphors and a short-wavelength excitation source.

Because of its distinctive photophysical characteristics, particularly in relation to the creation and amplification of light, lanthanide ions (Ln^{+3})occupy a special place in the field of photonics [4, 5]. Numerous scientific fields, from laser physics to molecular biology, have explored the luminescence Ln^{+3} and continue to do so. Samarium is one of the most interesting Ln+3 ions for studying fluorescence characteristics (4f5); Sm^{+3} emits highly sought-after red and orange emissions that are used in cathode ray tubes, photo-detectors, lasers, and prospective high-density optical storage applications as optical devices (e.g., color displays, optical data storage, televisions to LED light)[6−8]. Depending on the matrix, multiple mechanisms are involved in the decay of excited states in Sm+3.

Various wet chemical methods, such as coprecipitation, hydrothermal, sol-gel technology, and combustion method, have been developed for materials synthesis[9−12] . The sol-gel technology is widely used, and it is an effective process. The chosen host glass is designed to have high lanthanide ions solubility, moderate lower melting point, structure, and chemical stability, as well as outstanding transparency and lower phonon energy, in order to satisfy the required application with the appropriate optical qualities[13−15]. Sm^{+3}-doped silicates release visible emissions, particularly in the reddish-orange emission zone, and are therefore in high demand for potential applications such as traffic signs, decoration, and textile printing [16].

In the present study, the sol-gel method was adopted to prepare samarium ions-doped silica xerogel monoliths as hosts for intense emissions in the visible region in order to investigate the effects of ion concentrations on the luminescence properties. This is applicable in the use of such structures in the field of white light applications.

Experimental Part:

Tetraethylorthosilicate (TEOS, purity >98%), ethanol (C_2H_5OH, 99.0 %), deionized water catalyzed by hydrochloric acid (HCl, 0.15 M) and samarium chloride hexahydrate ($SmCl_3.6H_2O$, 99.9 % from Aldrich) with a molar ratio of 1:5:10 For TEOS/ethanol/water were used in the synthesis of undoped and/or doped silica xerogel monoliths with Sm^{+3} ions by the sol-gel technology.

Firstly, TEOS was mixed with ethanol and stirred for 30 min, then diluted HCl was added to the solution instead of pure water to catalyze the hydrolysis/condensation reactions. The mixture was stirred continuously for another 30 min. Sm^{+3} solutions of different concentrations were prepared by dissolving $SmCl_3.6H_2O$ in deionized water; 1 ml of these solutions with different concentrations (0.04, 0.09, 0.225, 0.55, 1.5) $\times 10^{-1}$ mol/l was added to the mixture and stirred for 30 min; this solution was left for 1 hour at room temperature. 0.5 ml of N, N dimethylformamide (C_3H_7NO), as a drying control chemical additive, was added to the final sol. By pouring the sol into a covered glass tube in an oven set at 60 °C, monoliths were able to gel. After 14 hours of ageing, the covers were removed to allow the solvent to evaporate throughout the drying process. At the end of the ageing period, the drying process

began by gradually increasing the temperature by 5 °C every 12 hours. The drying process went from 60 °C to 90 °C in 3 hours and then to 110 °C in 2 days. Transparent non-doped monoliths and monoliths with diameters of 0.7 to 0.8 cm, lengths of 1.9 to 2.1 cm, and weights of 1.1899 to 1.3932 gm and containing varying concentrations of Sm^{3+} ions: (4.3, 10.0, 21.9, 50.5, 178.0) $*10^{-4}$ % were successfully prepared.

Results and discussion:

 prepare samarium ions-doped silica xerogel monoliths

Figure (1) presents The X-ray diffraction patterns (XRD) of a non-doped and Sm^{+3} doped silica xerogel monoliths. The amorphous structure of the undoped silica sample is clearly observed. On the other side, the XRD pattern of doped samples showed a broad peak centered at $2\theta = 23.2°$, proving that the distribution of the activator ions (Sm^{+3}) in the SiO_2 network is random.
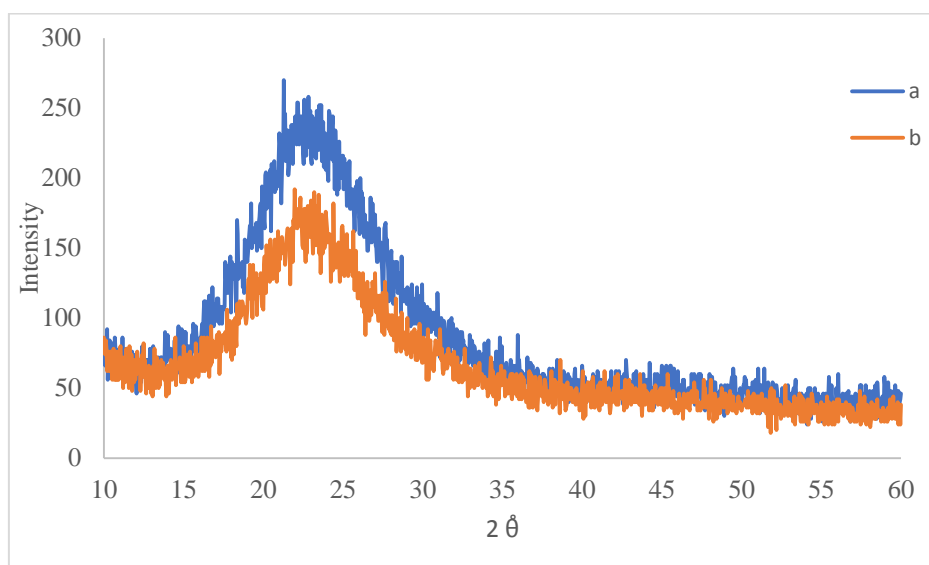

Figure.1: X-ray diffraction patterns of monoliths ;(a) non-doped monolith, (b) 0.0178% Sm^{+3} doped monolith

Fourier transform infrared (FTIR) spectra (using FTIR-spectrometer, Shimadzu, on KBr pellets of the samples at a resolution over the range $4000 – 400\ cm^{-1}$) of undoped silica xerogel monolith and one of the doped samples are shown in Figure (2). Five absorption bands that correspond to the host's characteristic vibrational bands are noted in the FTIR spectra; these bands were located at approximately $470\ cm^{-1}$, $800\ cm^{-1}$, and $1064\ cm^{-1}$, and were caused by the bending, symmetric stretching, and asymmetric stretching vibrations of siloxane Si-O-Si groups, respectively. While a weaker band at approximately $960\ cm^{-1}$ was caused by the stretching vibration of silanol Si-OH groups[17]. At roughly $1658\ cm^{-1}$ and $3419\ cm^{-1}$, two more bands developed. The O-H bond in water molecules vibrates in these two bands[17–19], showing that the drying process at 60 °C does not entirely capture the water molecules from the silica pores.
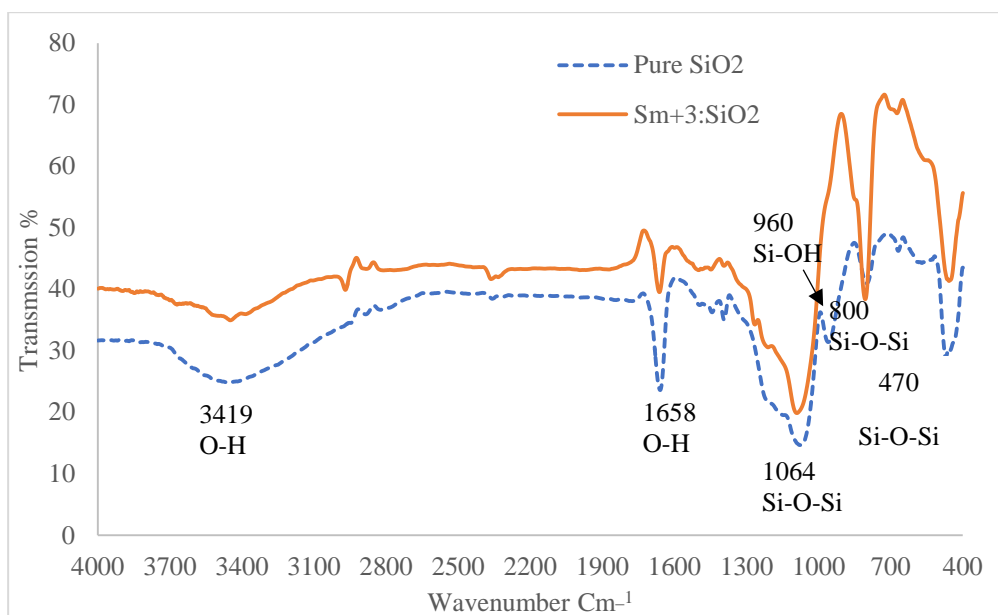
Figure 2: FTIR spectra of the undoped silica xerogel and Sm^{+3} doped silica xerogel.

The UV-Vis absorption spectra of Sm^{+3} ions in deionized water solutions were recorded with a Shimadzu UV–Vis Spectrophotometer, as shown in Figure (3). Several absorption bands caused by electronic transitions of the energy levels of Sm^{+3} ions were observed and located at about 305, 317, 332, 344, 362, 374, 390, 401, 415, 441, 463, 479 and 499 nm that corresponds to the transitions $^6H_{5/2} \rightarrow {}^3H_{9/2}, {}^4F_{11/2}, {}^4D_{7/2}, {}^3H_{7/2}, {}^4F_{9/2}, {}^4D_{5/2}, {}^6P_{7/2}, {}^4F_{7/2}, {}^6P_{5/2}, {}^4G_{9/2}, {}^4F_{5/2}, {}^4I_{11/2}$ and $^4G_{7/2}$, respectively [16–18]. Absorbance corresponding to these transitions depends on the samarium ions' concentration in a solution. It can be seen that as the concentration of Sm^{+3} increases, the absorbance bands become increasingly prominent and sharper. This is due to the increase of ions contribution in the absorption process so much as the increase of their concentrations according to Lambert–Beer's law.
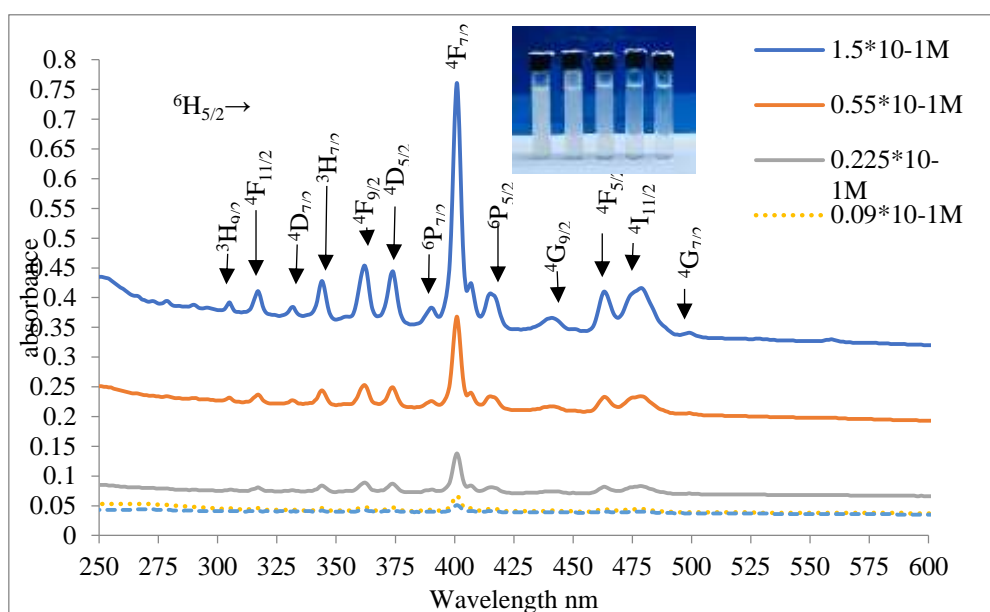

Figure 3: The absorption spectra of the samarium chloride hexahydrate in the deionized water.

Figure (4) illustrates the Sm^{+3} doped silica xerogel monoliths' absorption spectra at various concentrations (4.3, 10.0, 21.9, 50.5, 178.0) $*10^{-4}$ %. From the figure, it is clear that the absorbance spectra of the doped monoliths structure are similar to the absorbance spectra of the samarium chloride hexahydrate solutions, indicating that the spectroscopic activity corresponding to the Sm^{+3} ions, and absorbance increases with the increase in the concentration of samarium ions with a slight blue shift in the Sm^{+3} doped monoliths.
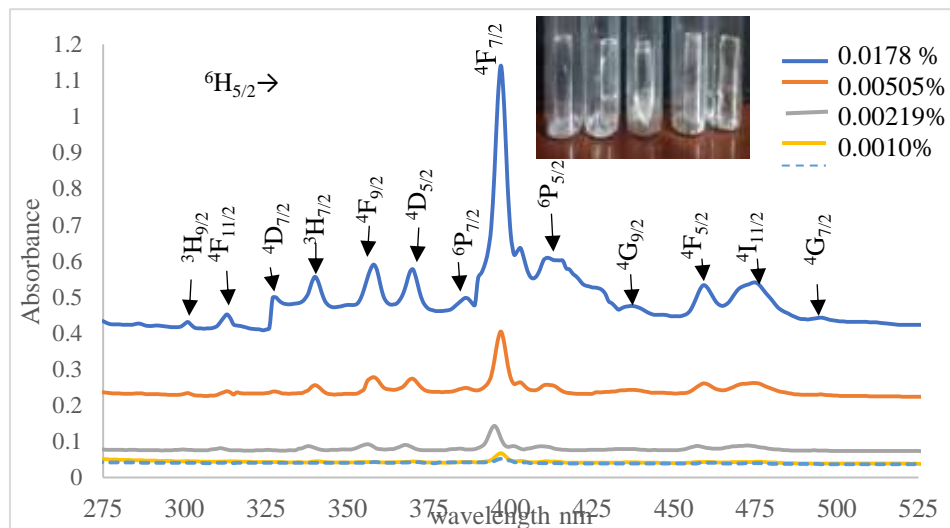

Figure 4: The absorption spectra of silica monoliths doped with different concentrations of Sm^{+3} ions.

The photoluminescence spectra of the samarium chloride hexahydrate solutions were registered with Shimadzu RF-5301 PC Spectrofluorophotometer, and 400 nm excitation wavelength of Xenon lamp as excitation source are exhibited in Figure (5). It was noticed that the emission peaks' intensity increased gradually with the increase in concentration from $0.004*10^{-1}$ M to $1.5*10^{-1}$ M of samarium chloride hexahydrate solution. The bands obtained in this present work are in agreement with previous investigations[20, 21]. The peaks at 562, 596, 647and 705 nm are assigned to a transition from the excited state $^4G_{5/2} \rightarrow {}^6H_J$ with J = 5/2; 7/2; 9/2 and 11/2 of Sm^{+3} ions, respectively[21–24] .
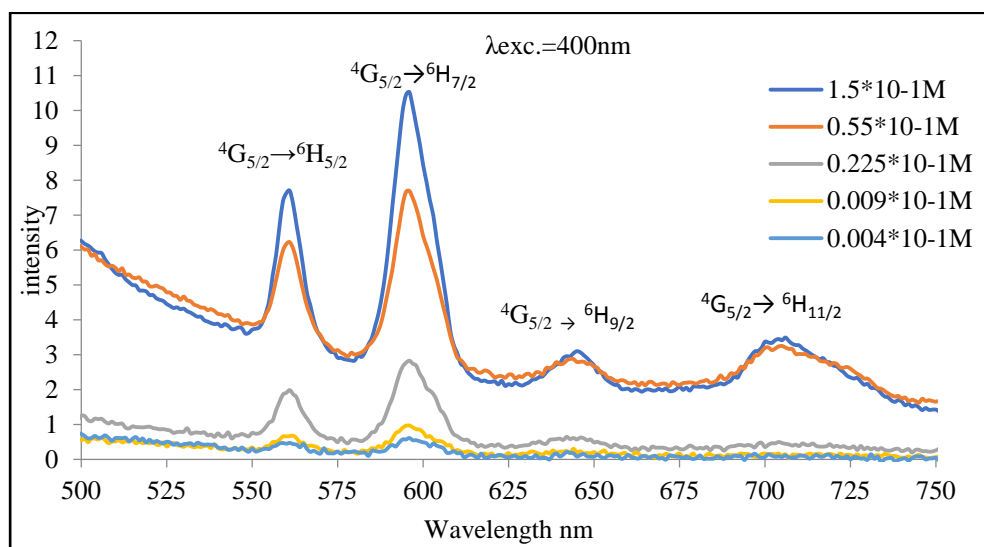

Figure 5: The emission spectra of samarium chloride hexahydrate in the deionized water, excited by 400 nm.

Figure (6) displays the photoluminescence spectra for the Sm^{+3} doped silica xerogel monolith with various Sm^{+3} ion concentrations under a 400 nm excitation wavelength. The Sm^{+3} intra-4f transition from excited levels to lower levels, represented by the $^4G_{5/2} \rightarrow {}^6H_{5/2}$ and $^4G_{5/2} \rightarrow {}^6H_{7/2}$ transitions, respectively, occurs at 569 nm and 601 nm in the yellow-orange region of the spectrum[21–24] . The $^4G_{5/2} \rightarrow {}^6H_{9/2}$ transition is the cause of another faint emission peak in the red region of spectra, which is positioned at 645 nm [20]. Electric-dipole transitions ($^4G_{5/2} \rightarrow {}^6H_{9/2}$), which emerge as a result of the absence of a center of symmetry, are produced, and their intensity is extremely sensitive to changes in the local structural environment of the Sm+3 ions. Although the magnetic-dipole permitted transitions $^4G_{5/2} \rightarrow {}^6H_{5/2}$ and $^4G_{5/2} \rightarrow {}^6H_{7/2}$ are seen, their strength rarely varies with the local structural symmetry of the Sm^{+3} ions[20, 21]. It is worth observing that the emission intensity is higher in the sample with a concentration of 0.00219 % than in the other samples. The occurrences of luminescence quenching for Sm^{+3} in the silica matrix that were observed in the other concentrations could be due to the energy transfer among the excited Sm^{+3} ions, such as the interaction between the lanthanide ions due to cross-relaxation (CR); strong interaction between two active ions transferring the excitation energy from one Sm^{+3} ion to another; O-H vibrations of water and concentration quenching exhibited by Sm^{+3} ions at higher concentrations [21]. This phenomenon is most likely caused by an increase in the number of nonradiative decay channels and also due to many closely spaced excited states, which leads to the quenching. It denotes the clustering of these ions within the pores of the sol-gel material.
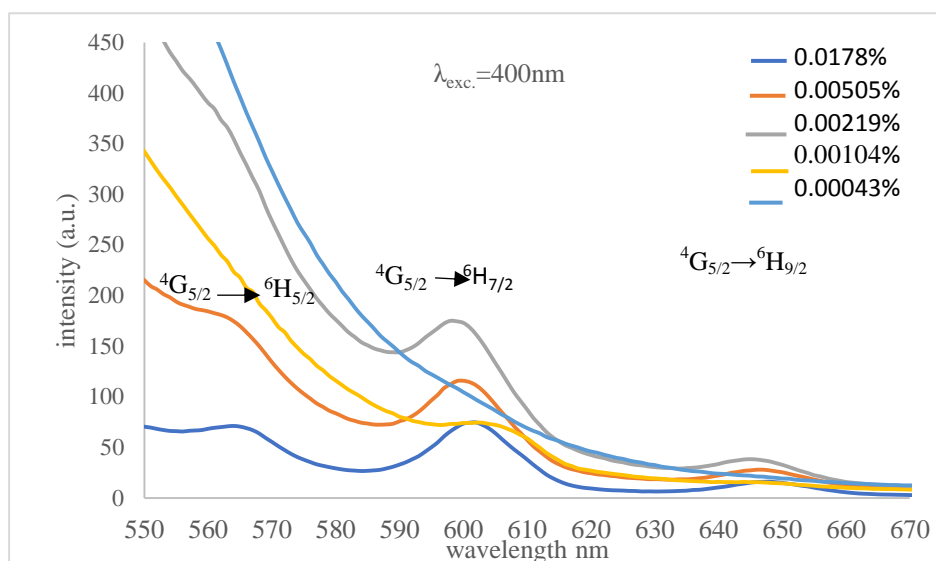

Figure 6: The emission spectra of silica monolith doped with different concentrations of Sm^{+3} ions, excited by 400 nm

From absorption spectra, absorption coefficients α(λ) and cross-sections σ (λ) spectroscopic parameters can be computed. The formula used to determine σ (λ) is [25] :

$$\sigma(\lambda) = \frac{\alpha(\lambda)}{\rho} \tag{1}$$

Where: ρ is the ion density (cm^3), the refractive index n(λ) was calculated with Michelson interferometer and was about (1.46-1.47). Bowen and Wokes gave an empirical formula to get a sufficiently accurate value of radiative lifetime τ_{rad} [26] :

$$1 / \tau_{rad} = 2.88 \times 10^{-9} \times n^2 * \grave{\upsilon} \int \varepsilon(\grave{\upsilon}) d\grave{\upsilon} \tag{2}$$

Where: υ is the wavenumber at the peak of the absorption band in cm^{-1}, $\int \varepsilon(\upsilon)d\upsilon$ is the area under the absorption band curve, and $\varepsilon(\upsilon)$ is the molecular extinction coefficient.

Peak emission cross-section (σ_{em}) for transtion $^4G_{5/2} \rightarrow {}^6H_{7/2}$ can be determined from:

$$\sigma_{em} = \frac{\lambda_p^4}{8\pi\,c\,\text{n`}^2\,\Delta\lambda_{eff}\,\tau_{rad}} \qquad (3)$$

Where: λ_p is a peak wavelength within the fluorescence band, $\Delta\lambda_{eff}$ is the emission linewidth (effective); which is determined by the Full Width Half Maximum (FWHM) of the emission band, and ń is given by:

$$\text{n`} = \frac{(n^2(\lambda)+2)^{\wedge}2}{9n(\lambda)} \qquad (4)$$

The oscillator strength f_{exp} can be calculated from the absorption spectra using the formula [2]:

$$fexp = 4.32 \times 10^{-9} \int \varepsilon(\upsilon)d\upsilon \qquad (5)$$

Table (1) includes the results of the calculated parameters from the recorder spectra. These parameters are related to the absorption band for the transition $^6H_{5/2} \rightarrow {}^4F_{7/2}$ and the emission band for the transition $^4G_{5/2} \rightarrow {}^6H_{7/2}$ of Sm^{+3} ions. Figure (7) displays the behavior of the oscillator strength f_{exp} and peak emission cross-section (σ_{em}) with different concentrations of Sm^{+3} ions in the doped samples. The values of oscillator strength of Sm^{+3} are connected with the hypersensitive electric dipole transitions indicating a non-symmetrical surrounding of Sm $^{+3}$ions in the silica network. Figure (7) indicates that the f_{exp} and σ_{em} vary with the Sm^{+3} ions concentration to reach a maximum value for the Sm^{+3} concentration of 0.00219 %, this behavior is due to the luminesces quenching.

Table 1: The spectroscopic parameters of silica xerogel monolith doped with Sm^{+3} ions.

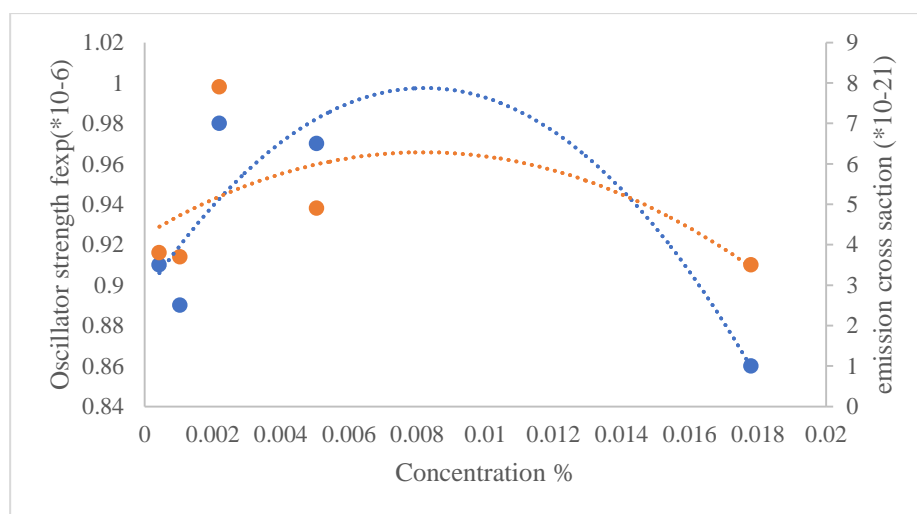| Sample no.	Ions concentration % Sm^{+3}	absorption cross-sections $\sigma(\lambda)$ ($\times10^{-20}$ cm^2)	Radiative lifetime τ_{rad} (ms)	oscillator strength $f_{exp}(\times10^{-6})$	Emission Cross section $\sigma_{em}(\times10^{-21}$ cm^2)
SSm1	0.00043	2.0	1.20	0.91	3.8
SSm2	0.00104	2.4	1.17	0.89	3.7
SSm3	0.00219	2.6	1.12	0.98	7.9
SSm4	0.00505	3.2	1.13	0.97	4.9
SSm5	0.0178	3.6	1.14	0.86	3.5

Figure 7: Variation in oscillator strength f_{exp} and peak emission cross-section (σ_{em}) with the concentrations of Sm^{+3} ions.

Conclusions:

Through the use of the sol-gel process, cylindrical and transparent silica xerogels monoliths that contain up to 0.0178% of samarium (Sm^{+3}) ions were successfully prepared. In these matrices, the structural behavior of these ions is described as being randomly distributed and incapable of forming any ligands in silica networks. These ions emit intense visible radiation. The spectroscopic analysis reveals that Sm^{+3} was clustering within the pores of the silica sol-gel host, which resulted in emission quenching at high doping levels. The current findings are viewed as a promising beginning for fields of study into the potential for improving the visible emissions of such ions through co-doping with metal nanoparticles like silver and gold that are beneficial in the white light-emitting diode (W-LED) applications.

References:

[1] V. Balaram, "Rare earth elements: A review of applications, occurrence, exploration, analysis, recycling, and environmental impact," *Geosci. Front.*, vol. 10, no. 4, pp. 1285–1303, 2019, doi: 10.1016/j.gsf.2018.12.005.

[2] M. A. Hamzah, M. A. Ameen, F. M. Mutar, and H. M. Yaseen, "Optical properties of Nd3+: SiO2 Prepared via Sol-Gel," *Int. J. Appl. or Innov. Eng. Manag.*, vol. 3, no. 5, 2014.

[3] B. T. Chiad, W. A. A. Twej, and F. J. Al-Maliki, "Synthesis of Nanosilica Glass Activated by Erbium Ions, Spectroscopic studies," *Iraqi J. Phys.*, vol. 7, no. 8, pp. 85–92, 2009.

[4] V. E. Ceniceros-Orozco, J. Escorcia-García, C. A. Gutiérrez-Chavarría, V. Agarwal, and H. U. López-Herrera, "Orange-reddish photoluminescence enhancement and wollastonite nanocrystals formation induced by CaO in Sm3+-doped calcium sodium borosilicate glasses," *Ceram. Int.*, vol. 48, no. 10, pp. 14537–14549, 2022.

[5] A. Jose, T. Krishnapriya, T. A. Jose, C. Joseph, and P. R. Biju, "Tunable luminescence and realization of warm white light via energy transfer from Dy3+/Er3+/Sm3+ triply doped glasses for photonic applications," *J. Lumin.*, vol. 236, p. 118105, 2021.

[6] A. Jose, T. Krishnapriya, T. A. Jose, C. Joseph, N. V Unnikrishnan, and P. R. Biju, "Color tunable luminescence characteristics and energy transfer analysis of Dy3+/Sm3+ co-doped multicomponent borosilicate glasses," *Scr. Mater.*, vol. 203, p. 114088, 2021.

[7] E. K. Papynov *et al.*, "Sol-gel and SPS combined synthesis of highly porous wollastonite ceramic materials with immobilized Au-NPs," *Ceram. Int.*, vol. 43, no. 11, pp. 8509–8516, 2017.

[8] E. K. Papynov *et al.*, "Synthetic CaSiO3 sol-gel powder and SPS ceramic derivatives:'In vivo' toxicity assessment," *Prog. Nat. Sci. Mater. Int.*, vol. 29, no. 5, pp. 569–575, 2019.

[9] X. Hou, Y. Zhang, H. Ding, and P. K. Chu, "Environmentally friendly wollastonite@ TiO2 composite particles prepared by a mechano-chemical method," *Particuology*, vol. 40, pp. 105–112, 2018.

[10] A. V. Deepa, M. Priya, and S. Suresh, "Influence of Samarium Oxide ions on structural and optical properties of borate glasses," *Sci. Res. Essays*, vol. 11, no. 5, pp. 57–63, 2016, doi: 10.5897/sre2015.6359.

[11] F. Hasan, "Synthesis of Cr Doped TiO2 Using Sol-Gel Technique and Calculation of its Photocatalytic Activity * Address for Correspondence Synthesis of Cr Doped TiO 2 Using Sol-Gel Technique and Calculation of its Photocatalytic Activity," no. June, 2019.

[12] D. B. Alwan, F. H. Ali, and W. A. A. Twej, "Improving the efficiency of dye-sensitized solar cells with doping and co-doping titanium dioxide," *Iraqi J. Sci.*, pp. 2228–2233, 2016.

[13] S. H. Hasan and S. S. M. Alawadi, "Reducing the Purification Period of Congo Red Dye Solution By Using Co-Exposure to Ultraviolet and Green Laser as A Photocatalysit Source," *Iraqi J. Sci.*, vol. 63, no. 5, pp. 2025–2038, 2022, doi: 10.24996/ijs.2022.63.5.18.

[14] S. S. AL-Awadi, R. T. Shbeeb, and B. T. Chiad, "Effect of silver nanoparticles on fluorescence spectra of C480 dye," *Iraqi J. Sci.*, vol. 59, no. 1 C, pp. 502–509, 2018, doi: 10.24996/IJS.2018.59.1C.7.

[15] F. J. Kadhim, W. A. A. Twej, T. S. Mahdi, and A. J. Majeed, "Photoluminescence analysis for terbium β-diketonate complex-based silica xerogel matrices," *J. Sol-Gel Sci. Technol.*, vol. 76, pp. 150–155, 2015.

[16] M. Monisha, M. I. Sayyed, N. Almousa, N. Karunakara, and S. D. Kamath, "Reddish-orange

emissions from Sm3+ doped zinc alumino borosilicate glasses: A correlative study on structural, thermal, and optical properties," *J. Non. Cryst. Solids*, vol. 586, no. May, p. 121568, 2022, doi: 10.1016/j.jnoncrysol.2022.121568.

[17] M. U. Khan, A. L. Fanai, and S. Rai, "Spectroscopic properties of Sm3+ and CdS co-doped in sol-gel silica glass," *Indian J. Pure Appl. Phys.*, vol. 58, no. 3, pp. 157–163, 2020, doi: 10.56042/ijpap.v58i3.25302.

[18] Z. Yang, D. Xu, and J. Sun, "Synthesis and luminescence properties of Ba 3 Lu (PO 4) 3: Sm 3+ phosphor for white light-emitting diodes," *Opt. Express*, vol. 25, no. 8, pp. A391–A401, 2017.

[19] W. A. A. Twej, B. T. Chiad, F. J. Al-Maliki, and A. J. H. Al-Wattar, "FTIR measurements for structural probing of rare-earth sol-gel silica glass system co-doped with Al3+," *2011 Int. Conf. Multimed. Technol. ICMT 2011*, no. October, pp. 6369–6373, 2011, doi: 10.1109/ICMT.2011.6002685.

[20] N. S. Jha, K. Linganna, C. K. Jayasankar, and A. K. Kar, "Sm3+ ions doped phosphate glasses for multiband visible laser applications," *Conf. Lasers Electro-Optics Eur. - Tech. Dig.*, vol. 2015-Augus, no. July, pp. 21–23, 2015, doi: 10.13140/RG.2.1.1445.1048.

[21] L. Van Vu, D. T. M. Huong, V. T. H. Yen, and N. N. Long, "Synthesis and optical characterization of samarium doped lanthanum orthophosphate nanowires," *Mater. Trans.*, vol. 56, no. 9, pp. 1422–1424, 2015, doi: 10.2320/matertrans.MA201526.

[22] M. J. Weber, "Faraday rotator materials for laser systems," in *Laser and Nonlinear Optical Materials*, SPIE, 1987, pp. 75–90.

[23] Z. Yang, D. Xu, J. Sun, Y. Sun, and H. Du, "Characterization and luminescence properties of Sr 3 Gd (PO 4) 3 : Sm 3 + orange–red phosphor," *Opt. Eng.*, vol. 54, no. 10, p. 105102, 2015, doi: 10.1117/1.oe.54.10.105102.

[24] M. Jayasimhadri, L. R. Moorthy, S. A. Saleem, and R. Ravikumar, "Spectroscopic characteristics of Sm3+-doped alkali fluorophosphate glasses," *Spectrochim. Acta Part A Mol. Biomol. Spectrosc.*, vol. 64, no. 4, pp. 939–944, 2006.

[25] O. B. Aljewaw *et al.*, "Impact of dy2o3 substitution on the physical, structural and optical properties of lithium–aluminium–borate glass system," *Appl. Sci.*, vol. 10, no. 22, pp. 1–17, 2020, doi: 10.3390/app10228183.

[26] C. A. Parker, *Photoluminescence of Solutions: with applications to photochemistry and analytical chemistry*. Elsevier Publishing Company, 1968.

NOTE: silica monolith, monolith, silica xerogel these different expression were used in different places in the paper, if they mean the same, they should be unified for clarity
Answer the note:
silica monolith, monolith, and silica xerogel all have the same meaning, it is unified in all the text body .